

Electromagnetic radiation in pp and Pb–Pb collisions with dielectrons in ALICE

Daiki Sekihata^{1,*}

¹Center for Nuclear Study, the University of Tokyo, 7-3-1 Hongo, Bunkyo, Tokyo, Japan, 113-0033

Abstract. In this article, final ALICE results on dielectron production, using the full data sample collected during the LHC Run 2, are presented. They include measurements of the dielectron and direct photon production in central Pb–Pb collisions at the center-of-mass energy per nucleon pairs $\sqrt{s_{NN}} = 5.02$ TeV, as well as minimum-bias and high-multiplicity pp collisions at $\sqrt{s} = 13$ TeV. First results with the Run 3 pp data at $\sqrt{s} = 13.6$ TeV, using the upgraded ALICE detector to disentangle the different dielectron sources, are also reported.

1 Introduction

Photons (γ) and dielectrons ($\gamma^* \rightarrow e^+e^-$) are emitted from all stages of the high-energy heavy-ion collision, and suffer negligible final-state interactions afterwards. Thus, they provide undistorted information at the time of their production. Drell-Yan pairs and prompt photons produced by the initial hard scattering are sensitive to the modification of nuclear parton distribution function (nPDF) in the colliding nuclei. Pre-equilibrium radiation reflects parton dynamics in the pre-equilibrium stage to study how quarks are produced from the initially purely gluonic system and how they reach equilibrium. Thermal radiation carries information on the thermodynamical properties and the space-time evolution of quark-gluon plasma (QGP) and hot hadronic matter. In addition, the m_{ee} spectrum is sensitive to chiral symmetry restoration via $\rho \rightarrow e^+e^-$ whose spectral function is modified in hot matter.

One of the advantages of dielectron measurement is that sources can be separated by the e^+e^- invariant mass. In the low mass region (LMR: $m_{ee} < 1.1$ GeV/ c^2), thermal radiation from the hot hadronic matter (e.g. $\pi^+\pi^- \rightarrow \rho\gamma^{(*)}$, $\pi^\pm\rho \rightarrow \pi^\pm\gamma^{(*)}$) is dominant. In the intermediate mass region (IMR: $1.1 < m_{ee} < 2.7$ GeV/ c^2), thermal radiation from the QGP (e.g. $q\bar{q} \rightarrow e^+e^-$, $qg \rightarrow q\gamma^{(*)}$, $q\bar{q} \rightarrow g\gamma^{(*)}$) is dominant. However, experimentally, these signals compete with dielectrons from hadron decays.

2 Final results on dielectrons from Run 2

2.1 Measurements of direct photons with the virtual photon technique in the LMR

ALICE has measured direct photons with the virtual photon technique. This technique was originally invented by PHENIX [1] at RHIC. The direct photon fraction $r = \gamma^{\text{dir}}/\gamma^{\text{inc}}$ as a function of p_T is extracted from the m_{ee} spectrum based on a template fit with three components consisting of light-flavor hadron decays (f_{LF}), heavy-flavor hadron decays (f_{HF}) and

*e-mail: daiki.sekihata@cern.ch

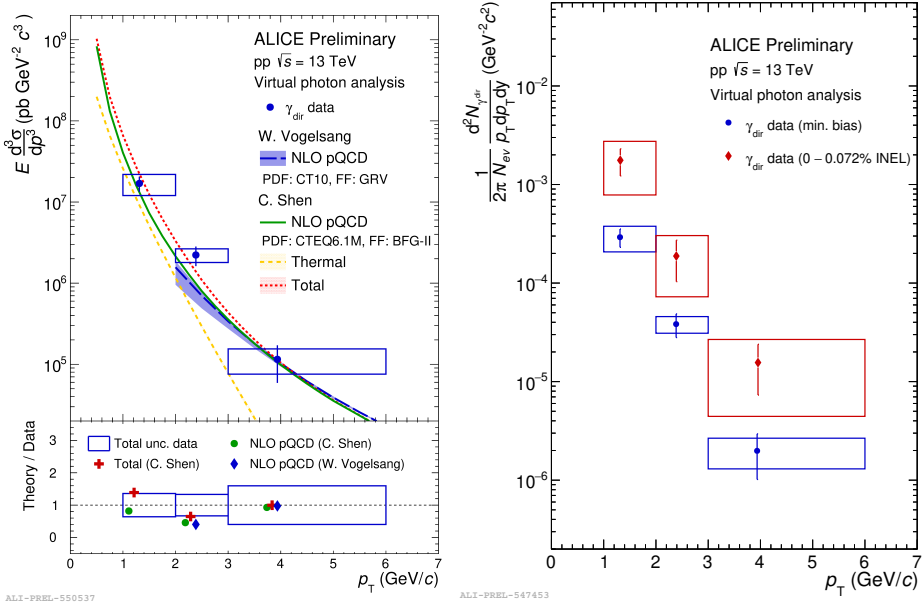


Figure 1. Left: The p_T spectrum of direct photons in minimum-bias pp collision at $\sqrt{s} = 13$ TeV compared with theoretical calculations [3]. Right: The p_T spectrum of direct photons in minimum-bias (blue) and high-multiplicity (red) pp collision at $\sqrt{s} = 13$ TeV.

dielectron productions associated with real photons (f_{dir}) given by Kroll-Wada formula [2]. The ratio of direct to inclusive photons is the same for real and virtual photons at the massless limit ($m_{ee} \rightarrow 0$ or $m_{ee} \ll p_{T,ee}$). The total fitting function f_{fit} is defined as

$$f_{\text{fit}} = r \times f_{\text{dir}} + (1 - r) \times f_{\text{LF}} + f_{\text{HF}}. \quad (1)$$

The only free parameter r is interpreted as the direct photon fraction. Fitting the m_{ee} spectrum above the π^0 mass allows us to reduce its background and the systematic uncertainties compared with the real direct photon measurement. Figure 1 (left) shows the p_T spectrum of direct photons in minimum-bias pp collision at $\sqrt{s} = 13$ TeV compared with theoretical calculations [3]. Data points are described by both prompt-only scenario and scenario with prompt + thermal photon from QGP droplet in small systems within our experimental uncertainties. In addition to the minimum-bias data, Figure 1 (right) shows the p_T spectrum of direct photons in high-multiplicity pp collision at $\sqrt{s} = 13$ TeV. The corresponding charged particle multiplicity at midrapidities for the two samples are $dN_{\text{ch}}/d\eta|_{\eta=0} \approx 7$ and 30 respectively. It is challenging to calculate the direct photon production in pp collisions currently from theory side. Hence, these measurements are critical inputs to theoretical calculations. In these years, it is found that high-multiplicity pp collisions interestingly exhibit similar phenomena to those in heavy-ion collisions. Direct photons provide interesting insights to underlying physics in such collisions, especially about searching for possible thermal radiation.

ALICE recently published results [4] about direct photon production in central Pb–Pb collisions. There, ALICE data points are compared with a state-of-the-art model [5] which includes prompt, pre-equilibrium, and thermal photons. The data points are described by the model within the experimental uncertainties, but the model tends to overestimate ALICE data by $\sim 1\sigma$.

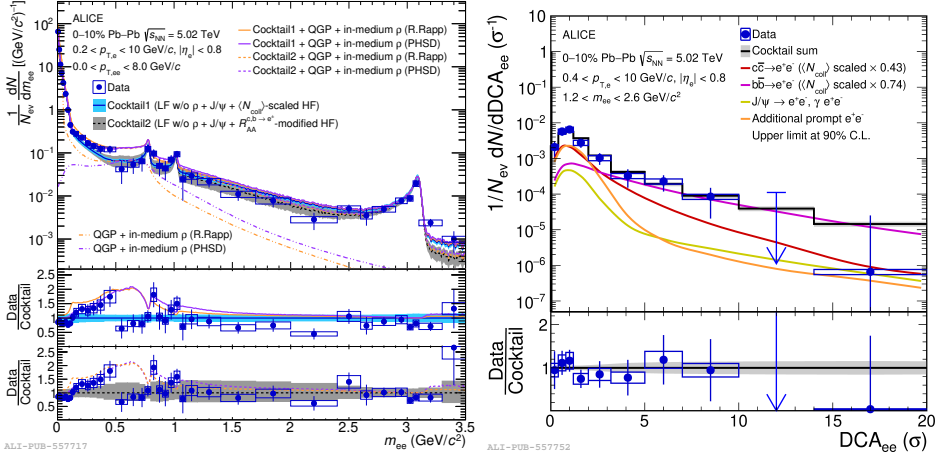


Figure 2. Left: Dielectron invariant mass m_{ee} spectrum compared with two theoretical models [9, 10] in central Pb–Pb collisions at $\sqrt{s_{NN}} = 5.02$ TeV. Right: Dielectron pair DCA (DCA_{ee}) spectrum and template fit with charm, beauty, and thermal contributions in central Pb–Pb collisions at $\sqrt{s_{NN}} = 5.02$ TeV.

2.2 Thermal dielectron production in the IMR

In the IMR, correlated e^+e^- pairs from semileptonic decays of open HF hadrons and thermal radiation from the partonic phase contribute to the m_{ee} spectrum. The correlated e^+e^- pairs from open HF hadrons are sensitive to parton energy-loss in the QGP. Figure 2 (left) shows the dielectron mass spectrum compared to two different estimates of the multi-component distributions, the so-called *cocktails*. Cocktail1 contains LF and N_{coll} -scaled HF components [6]. Cocktail2 consist of LF and HF cocktail modified by the R_{AA} of single electrons from HF hadron decays [7, 8] in order to take shadowing and energy loss for heavy quarks into account. Cocktail1 shows agreement with data, but is at the edge of uncertainties. While Cocktail2 shows improvement, the cocktail uncertainty in the IMR increases due to the modification. This comparison tells that a cocktail-independent method is necessary to extract thermal radiation from the QGP. ALICE performed the first topological separation between thermal radiation (prompt) and dielectrons from HF hadron decays (non-prompt) in central Pb–Pb collisions. While thermal dielectrons are produced promptly at the primary vertex, electrons from HF hadron decays have larger distance of closest approach to the primary vertex (DCA) because of long life time for charmed hadrons ($c\tau \sim 150 \mu\text{m}$ for D meson family and $60 \mu\text{m}$ for Λ_c^+). Figure 2 (right) shows the DCA_{ee} spectrum and template fit with charm, beauty, and thermal contributions in central Pb–Pb collisions at $\sqrt{s_{NN}} = 5.02$ TeV. To obtain the best fit, charm and beauty contributions are scaled down by a factor of 0.43 and 0.74 respectively, and thermal contribution is scaled up by a factor of 3.17. Currently, statistical uncertainty is dominant in ALICE data points [4]. Nevertheless, the DCA analysis is promising and becomes important in Run 3.

3 First results on dielectrons from Run 3

ALICE collected high statistics in pp collisions at $\sqrt{s} = 13.6$ TeV in 2022 and 2023. Figure 3 (left) shows the raw invariant mass spectrum with 1 pb^{-1} of the pp data in 2022. The ω/ρ , ϕ , J/ψ , $\psi(2S)$, $\Upsilon(1S)$ peaks and HF continuum in the intermediate and high mass region are visible. Figure 3 (right) shows the raw m_{ee} spectrum with smaller (blue) and larger (red) DCA_{ee} selections. There is only the HF continuum and a small peak of non-prompt J/ψ with

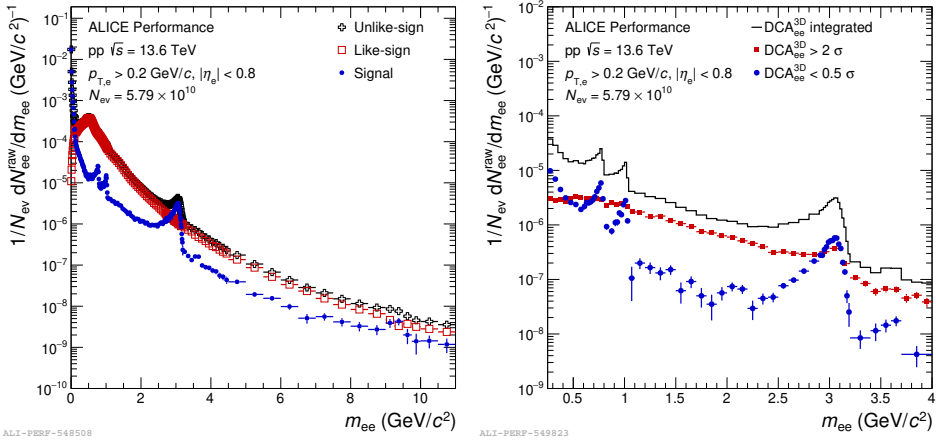


Figure 3. Left: Raw invariant mass m_{ee} spectrum in pp collisions at $\sqrt{s} = 13.6$ TeV together with unlike-sign and like-sign distributions. Right: Raw invariant mass m_{ee} spectrum with different DCA_{ee} selections in pp collisions at $\sqrt{s} = 13.6$ TeV.

larger DCA_{ee} selection. On the other hand, the vector meson peaks are pronounced with smaller DCA_{ee} selection. These first results show strong separation power of DCA between thermal radiation and dielectrons from HF hadron decays in Run 3.

4 Summary and Outlook

ALICE has measured dielectrons and direct photons with the virtual photon technique from small to large systems at the LHC energies. Direct photon production at low p_T in pp collisions at $\sqrt{s} = 13$ TeV is described by prompt-only and prompt + thermal photon scenarios within experimental uncertainties. This serves as crucial input to theoretical calculations in the non-perturbative regime. Direct photon production in central Pb–Pb collisions at $\sqrt{s_{NN}} = 5.02$ TeV is described by the latest model. But, the model tends to overestimate ALICE data by $\sim 1\sigma$. The first results of DCA analysis in pp collisions at $\sqrt{s} = 13.6$ TeV show strong separation power between prompt and non-prompt dielectron sources.

References

- [1] A. Adare et al. (PHENIX), Phys. Rev. C **81**, 034911 (2010), 0912.0244
- [2] N.M. Kroll, W. Wada, Phys. Rev. **98**, 1355 (1955)
- [3] C. Shen, J.F. Paquet, G.S. Denicol, S. Jeon, C. Gale, Phys. Rev. C **95**, 014906 (2017), 1609.02590
- [4] S. Acharya et al. (ALICE) (2023), 2308.16704
- [5] C. Gale, J.F. Paquet, B. Schenke, C. Shen, Phys. Rev. C **105**, 014909 (2022), 2106.11216
- [6] S. Acharya et al. (ALICE), Phys. Rev. C **102**, 055204 (2020), 2005.11995
- [7] S. Acharya et al. (ALICE), Phys. Lett. B **804**, 135377 (2020), 1910.09110
- [8] K.J. Eskola, H. Paukkunen, C.A. Salgado, JHEP **04**, 065 (2009), 0902.4154
- [9] R. Rapp, Adv. High Energy Phys. **2013**, 148253 (2013), 1304.2309
- [10] T. Song, W. Cassing, P. Moreau, E. Bratkovskaya, Phys. Rev. C **97**, 064907 (2018), 1803.02698